Pergamon

Tetrahedron, Vol. 52, No. 39, pp. 12651-12666, 1996

0040-4020/96 $15.00 + 0.00

PII: S0040-4020(96)00737-5

Novel Mammalian Cell Cycle Inhibitors, Spirotryprostatins A and B, Produced by *Aspergillus fumigatus*, Which Inhibit Mammalian Cell Cycle at G2/M Phase[1)]

Cheng-Bin Cui, Hideaki Kakeya and Hiroyuki Osada*

The Institute of Physical and Chemical Research (RIKEN),
Hirosawa 2-1, Wako-shi 351-01, Saitama, Japan

Abstract: Two novel diketopiperazine alkaloids, spirotryprostatins A and B, were isolated as new inhibitors of the mammalian cell cycle from the secondary metabolites of *Aspergillus fumigatus* through a separation procedure guided by cell cycle inhibitory activity. The structures of spirotryprostatins A and B were determined by spectroscopic methods especially by detailed analyses of their ^{1}H and ^{13}C NMR spectra with the aid of 2D NMR techniques. Spirotryprostatins A and B had a novel structural skeleton with an unique spiro ring system and inhibited the cell cycle progression of tsFT210 cells at the G2/M phase with IC_{50} values of 197.5 μM and 14.0 μM, respectively.

As products of oncogenes and tumor suppressor genes are involved in the regulation of mammalian cell cycle[2-3)] and also as cancers in fact are the uncontrolled cell proliferation with deregulation of cell cycle[4)], new cell cycle inhibitors might be good candidates for cancer chemotherapy and also be a source for providing molecular probes useful in elucidating regulatory mechanism of the cell cycle[5)]. We have therefore begun on the screening for new cell cycle inhibitors from microbial origin[5-9)]. During the screening, we have previously reported three new natural diketopiperazines, tryprostatins A, B and demethoxyfumitremorgin C, together with four known diketopiperazines, fumitremorgin C, 12,13-dihydroxyfumitremorgin C, fumitremorgin B and verruculogen, as a new group of M-phase inhibitors of the mammalian cell cycle, which were isolated from the fermentation broth of a fungus, *Aspergillus fumigatus*[6,8,9)].

In the continuation of that work, in order to obtain larger amounts of those compounds to examine their biological activities in detail, we carried out a large scale fermentation of the producing strain. From the fermentation broth, we have now isolated two novel diketopiperazine alkaloids, spirotryprostatins A (**1**) and B

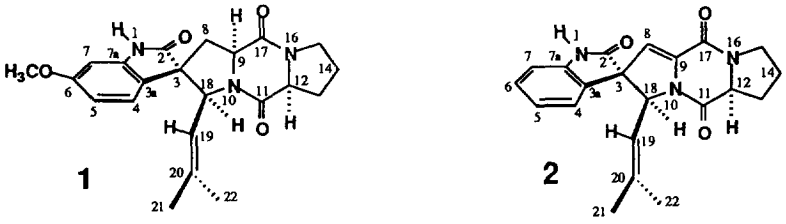

Chart 1 Structures of Spirotryprostatins A (**1**) and B (**2**).

(2), together with the former four compounds in a larger quantity through a separation procedure guided by inhibitory activity on the cell cycle progression of mouse tsFT210 cells. Both the compounds **1** and **2** inhibited the cell cycle progression of tsFT210 cells at the G2/M phase. In this paper, we mainly describe the isolation, structure determination and biological activities of **1** and **2**.

Fermentation and Isolation

The producing strain was cultured in a 600-liter jar fermenter containing 400 liters of fermentation medium (glucose 3%, soluble starch 2%, soybean meal 2%, K_2HPO_4 0.5% and $MgSO_4 \cdot 7H_2O$ 0.05%, adjusted at pH 6.5 before sterilization) containing 0.05% of CA-123 and KM-68 antifoam, respectively. The fermentation was carried out at 28°C for 66 hours under 350 rpm stirring speed and 200 liters/minute aeration rate.

The whole broth was filtrated to separate to a broth supernatant (370 L) and a mycelial cake. The latter was extracted with 90% aqueous acetone which was evaporated *in vacuo* to remove acetone. Both the broth supernatant and the mycelium extract (60 L) were extracted respectively with EtOAc. The EtOAc solutions obtained were combined and concentrated *in vacuo* to afford an oily extract (1.2 L) which was further purified as shown in Fig. 1 to give an active extract (66 g). This extract was then separated by a combination of silica gel column chromatography, middle pressure liquid chromatography and repeated HPLC (CAPCELL PAK C-18 and CAPCELL PAK C-8, Shiseido) to give **1** (1.2 mg) and **2** (11 mg) (Fig. 1), respectively, together with tryprostatins A (1048 mg), B (64.4 mg), demethoxyfumitremorgin C (159.6 mg) and fumitremorgin C (903.5

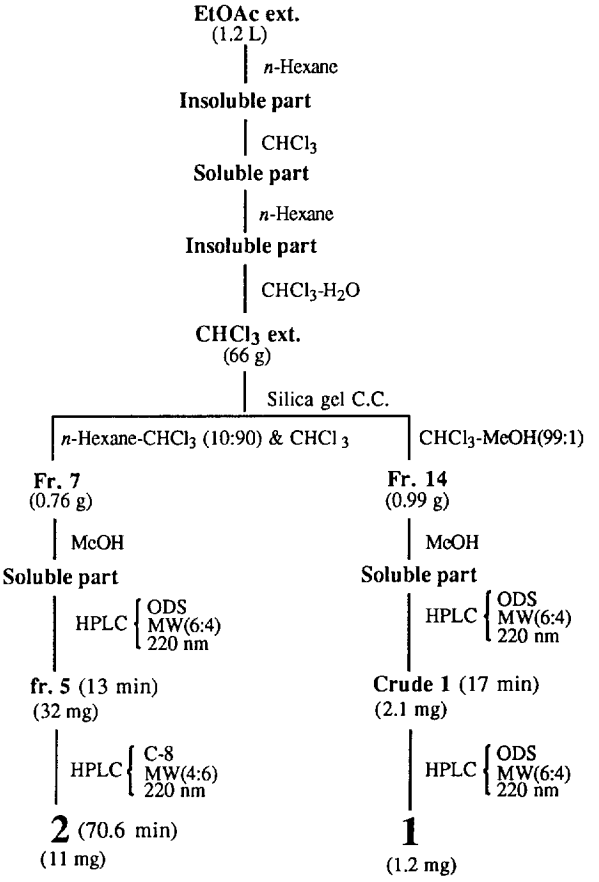

Fig. 1. Isolation Procedure for **1** and **2**.
MW is the abbreviation of MeOH-Water.

mg). The latter four compounds were identified by direct comparison with authentic samples[9], respectively.

Physico-chemical Properties of Spirotryprostatins A (1) and B (2)

Both spirotryprostatins A (**1**) and B (**2**) were obtained as slightly yellow-colored forms and their physico-chemical properties are summarized in Table 1.

Table 1. Physico-chemical Properties of Spirotryprostatins A (**1**) and B (**2**).

Characteristics	**1**	**2**
Appearance	Pale Yellow Amorphous Powder	Pale Yellow Crystalline Solid
MP	——	137-138°C
$[\alpha]_D$ in $CHCl_3$	$[\alpha]_D^{26}$ -34.0°(c 0.10)	$[\alpha]_D^{22}$ -162.1°(c 0.92)
Molecular Formula	$C_{22}H_{25}N_3O_4$	$C_{21}H_{21}N_3O_3$
Molecular Weight	395	363
EI-MS *m/z*	395 (M^+, 100%), 220 (58%)	363 (M^+, 100%), 266 (60%)
HR-EI-MS	M^+	M^+
Found (*m/z*)	395.1804	363.1612
Calcd (*m/z*)	395.1801	363.1609
UV λ_{max}^{MeOH} nm (ε)	219 (15920), 245 (sh, 4400), 270 (3020), 280 (sh, 2960)	212 (36660), 227 (sh, 28820), 242 (sh, 24830), 272 (sh, 17350), 286 (sh, 14810)
IR ν_{max}^{KBr} cm^{-1}	3430, 3270 (NH), 2970, 2935, 2880, 2850 (CH_3 & CH_2), 1715 (γ-lactam C=O), 1680, 1665 (amide C=O), 1635, 1480, 1425, 755	3440, 3240 (NH), 2970, 2930, 2870, 2860 (CH_3 & CH_2), 1730 (γ-lactam C=O), 1680, 1655 (amide C=O), 1640 (C=C), 1470, 1420, 750

Structural Elucidation for Spirotryprostatin A (1)

Spirotryprostatin A (**1**) was obtained as a pale yellow amorphous powder and showed $[\alpha]_D$ -34.0° ($CHCl_3$). The molecular formula of **1** was determined to be $C_{22}H_{25}N_3O_4$ by HR-EI-MS measurement (Found 395.1804 (M^+), calcd for $C_{22}H_{25}N_3O_4$ 395.1801), which was well consistent with its ^1H and ^{13}C NMR data (Table 2). In the UV spectrum, **1** showed absorption maxima ascribable to a substituted benzene ring at 219 (ε 15920) and 270 nm (3020), and the IR spectrum of **1** showed absorption bands at 3430, 3270 (NH), 2970, 2935, 2880, 2850 (CH_3 and CH_2), 1715 (γ-lactam C=O), 1680 and 1665 cm^{-1} (amide C=O) in the functional group region.

In the ^1H NMR spectrum, **1** showed signals due to an N-H proton (δ7.64 br s, 1-H), an 1,2,4-trisubstituted benzene ring (δ6.93 d, J=8.5 Hz, 4-H; δ6.50 dd, J= 8.5, 2.4 Hz, 5-H; and δ6.43 d, J=2.4 Hz, 7-H), an olefinic proton (δ5.03 dm, J=10.0 Hz, 19-H) and a methoxy (δ3.80 s, $OC\underline{H}_3$) and two methyl (δ1.65 s, 21-$\underline{H}_3$ and δ1.26 s, 22-$\underline{H}_3$) groups along with signals due to several methine and methylene groups (Table 2). The ^{13}C NMR spectrum of **1**, analyzed by the DEPT method, indicated the presence of three amide carbonyls

(δ180.86 s, C-2; δ167.07 s, C-11; and δ166.94 s, C-17), an oxygen-bearing sp^2 carbon (δ160.37 s, C-6) and a methoxy (δ55.46 q, O<u>C</u>H$_3$) and two methyl (δ25.50 q, C-21 and δ17.98 q, C-22) groups together with four sp^2 and three sp^3 methines, three sp^2 and a sp^3 quaternary carbons, and three methylene groups (Table 2).

Table 2. 400 MHz ^{1}H and 100 MHz ^{13}C NMR data for Spirotryprostatin A (**1**) in chloroform-*d*[a)]

Positions	δ_H (*J* in Hz)	NOE's[b)]	δ_c	HMBC	
				2-bonds[c)]	3-bonds[d)]
1 (N<u>H</u>)	7.64 br s	7	-------		
2	----		180.86[e)] s		8α, 18
3	----		59.99 s	8β	
3a	----		118.70 s		5, 7
4	6.93 d (8.5)	5, 19	127.24 d		
5	6.50 dd (8.5, 2.4)	4, OCH$_3$	106.77 d		7
6	----		160.37 s	7	4, OCH$_3$
7	6.43 d (2.4)	1, OCH$_3$	96.66 d		5
7a	----		141.68 s		4
8α	2.39 dd (13.2, 6.8)	8β, 9	34.30 t		
β	2.60 dd (13.2, 10.5)	4, 8α, 19			
9	4.99 dd (10.5, 6.8)	8α, 12, 18	58.47 d	8β	
11	----		167.07[f)] s		
12	4.28 dd (8.3, 7.8)	8α, 9	61.02 d		
13	2.27 m		27.41 t	12	
	2.31 m				
14	1.97 m		23.64 t		
	2.07 m				
15	3.57 m		45.18 t		
	3.61 m				
17	----		166.94[g)] s		
18	4.78 d (10.0)		60.15 d		8β
19	5.03 dm (10.0)	4	121.30 d	18,	21, 22
20	----		138.39 s	21, 22	
21	1.65 s	19, 22	25.50 q		19, 22
22	1.26 s	18, 21	17.98 q		19, 21
OCH$_3$	3.80 s	5, 7	55.46 q		

a): Signal assignments were based on the results of ^{1}H-^{1}H COSY, PFG-HMQC, PFG-HMBC and difference NOE experiments. b): Numbers in the column indicate the protons at which NOE's were observed in the difference NOE experiment under irradiation of the proton in the corresponding line. c) and d): Numbers in each column respectively indicate the protons coupled with the carbon through two and three bonds, respectively, which were detected in the PFG-HMBC spectrum. e): Signal assignment was based on a comparison with the data (Table 3) of **2**. f) and g): Signal assignments were based on a comparison with the data of tryprostatins and related diketopiperazine derivatives[6,9].

The amide carbonyl absorption at 1680 and 1665 cm^{-1} together with the absence of the amide II band near 1550 cm^{-1} in the IR spectrum suggested the presence of a diketopiperazine system[7,9] in **1**. This was further supported by the amide carbonyl carbon signals at δ167.07 and δ166.94 (C-11 and C-17) in the ^{13}C NMR spectrum, which were assignable to the carbonyls in the diketopiperazine system[9]. The carbonyl absorption at 1715 cm^{-1} in the IR spectrum, coupled with the ^{13}C signal of the carbonyl carbon at δ180.86 (C-2) in the ^{13}C NMR spectrum, revealed the existence of a γ-lactam moiety fused to an aromatic ring[1,10] in **1**.

Detailed analyses of the ^{1}H and ^{13}C NMR spectra of **1** with the aid of pulse field gradient (PFG) ^{1}H-^{1}H COSY and PFG heteronuclear multiple quantum coherence (PFG-HMQC) spectroscopy, coupled with the results of difference NOE experiments and the above structural information, enabled us to deduce partial structures A, B and C (Fig. 2) in **1**.

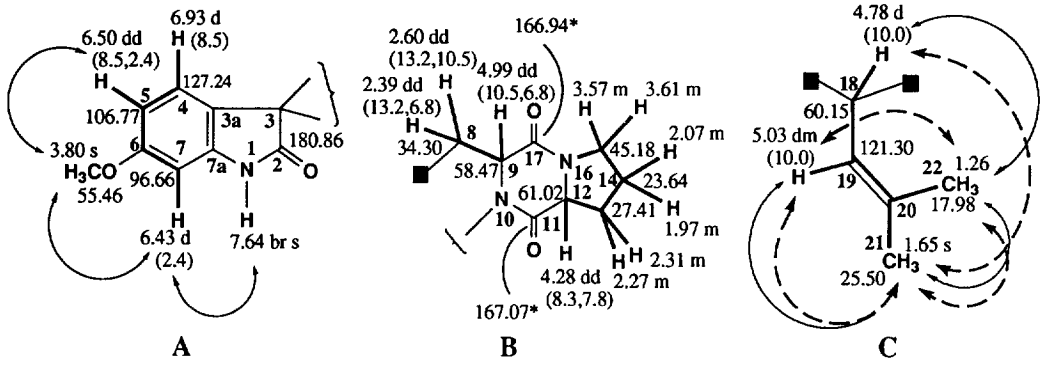

Fig. 2. Partial structures, A, B and C, and NMR data for **1**

Bold lines indicate spin systems obtained by the analyses of ^{1}H-^{1}H COSY and PFG-HMQC spectra. Dashed line arrows indicate long-range ^{1}H -^{1}H couplings observed in the ^{1}H-^{1}H COSY. Solid line arrows indicate NOE's observed in the difference NOE experiments. *Signals were assigned by comparison with the data of tryprostatins and related diketopiperazine derivatives[6,9].

Then, the PFG heteronuclear multiple bond correlation (PFG-HMBC) spectrum was measured in order to determine total structure of **1**. In the PFG-HMBC spectrum (Table 2), the oxygen-bearing quaternary *sp*^{2} carbon at δ160.37 (C-6) showed long-range correlations with the benzene protons 4-H (δ6.93) and 7-H (δ6.43) and the methoxy protons at δ3.80 ($OC\underline{H}_3$) in the partial structure A, while the quaternary *sp*^{2} carbons at δ118.70 (C-3a) and at δ141.68 (C-7a) showed long-range correlations with 5-H (δ6.50) and 7-H and with 4-H in the partial structure A, respectively. Therefore, they were assigned respectively to C-6 (δ160.37), C-3a (δ118.70) and C-7a (δ141.68) in the partial structure A. The γ-lactam carbonyl carbon (δ180.86, C-2) could be assigned by comparison with the data of **2**, which were exhaustively analyzed and assigned exactly by direct information

from NMR studies (see below). For the partial structure B, the PFG-HMBC spectrum did not give satisfactory long-range correlations to assign the signals for the amide carbonyls because of the scarcity of the sample. However, two carbonyl carbons at δ167.07 and δ166.94 could be assigned to the amide carbonyl carbons C-11 and C-17 in the partial structure B, respectively, by a comparison of their chemical shift values with those of tryprostatins and other related diketopiperazine derivatives[6,9]. As to the partial structure C, the quaternary sp^2 carbon at δ138.39 could be assigned to C-20, which showed long-range correlations with 21-$\underline{H}_3$ (δ1.65) and 22-$\underline{H}_3$ (δ1.26) in PFG-HMBC spectrum. Signal assignments for those quaternary sp^2 carbons are summarized in Table 2.

Next, in the PFG-HMBC spectrum (Table 2), both 8-H_α (δ2.39) in the partial structure B and 18-H (δ4.78) in the partial structure C showed long-range correlations with the C-2 carbonyl carbon (δ180.86) in the partial structure A, while the 8-H_β (δ2.60) in the partial structure B correlated with the C-18 carbon (δ60.15) in the partial structure C and the sp^3 quaternary carbon at δ59.99 (C-3, in the partial structure A). Therefore, C-8 in the partial structure B and C-18 in the partial structure C could be connected across the C-3 carbon in the partial structure A, and the quaternary carbon at δ59.99 could be assigned to C-3. At this stage, from a consideration of the chemical shift of C-18 (δ60.15) and the molecular formula of **1**, $C_{22}H_{25}N_3O_4$, coupled with its unsaturation numbers (among 12 in **1**, 11 have been counted at this stage), C-18 could be linked to the nitrogen atom at the position 10 to form a five-membered spiro ring in **1**. Thus the planar structure of **1** was deduced.

The relative stereochemistry of **1** was determined by difference NOE experiments in where significant NOE's were observed between 12-H, 9-H and 8-H_α (δ2.39) and between 19-H, 8-H_β (δ2.60) and 4-H, respectively (Table 2). This means that the protons 18-H, 12-H, 9-H and 8-H_α in **1** are all in the *cis*-relations and the protons 4-H, 8-H_β and 19-H should be oriented in the same direction in **1**. Therefore, the relative stereochemistry of spirotryprostatin A were determined as shown by the formula **1** in Chart 1. Some other NOE's observed in the difference NOE experiments and long-range ^1H-^{13}C couplings detected in the PFG-HMBC spectrum are summarized in Table 2.

Structural Elucidation for Spirotryprostatin B (2)

Spirotryprostatin B (**2**) was obtained as a slightly yellow-colored crystalline solid having melting point 137-138°C and showed $[\alpha]_D$ -162.1° ($CHCl_3$). The molecular formula of **2** was determined to be $C_{21}H_{21}N_3O_3$ by HR-EI-MS measurement (Found 363.1612 (M^+), calcd for $C_{21}H_{21}N_3O_3$ 363.1609), coupled with its ^1H and ^{13}C NMR data (Table 3). The UV spectrum of **2** showed characteristic absorption bands spread broadly over the 200-310 nm region[1], with the absorption maxima at 212 (ε 36660), 227 (sh, 28820), 242 (sh, 24830) 272 (sh, 17350) and 286 nm (sh, 14810). This might be ascribed to the substituted benzene ring and the α,β-unsaturated carbonyl system in **2**. The IR spectrum of **2** revealed, like that of **1** (Table 1), the presence of a γ-lactam fused to an aromatic ring with the absorption bands at 3440, 3240 (NH) and 1730 cm^{-1} (γ-lactam C=O), the presence of methyl and methylene groups with 2970, 2930, 2870 and 2860 cm^{-1} and the presence of a diketopiperazine

system with the amide carbonyl absorptions at 1680 and 1655 cm^{-1} together with the absence of amide II band near 1550 cm^{-1} in the functional group region.

The ^1H and ^{13}C NMR spectra of **2** (Table 3), in which the methoxy signals (δ_H3.80 s and δ_C55.46 q) in **1** have been disappeared, showed slightly different signal patterns compared with those of **1**, probably because of the introduction of a double bond forming an enamine moiety fused to diketopiperazine skeleton[11]. In the ^1H NMR spectrum, **2** showed signals due to an N-H proton (δ8.67 br s, 1-H), an 1,2-disubstituted benzene ring (δ7.06 br d, *J*=7.6 Hz, 4-H; δ6.99 td, *J*= 7.6, 1.0 Hz, 5-H; δ7.23 td, *J*=7.6 1.0 Hz, 6-H and δ6.89 br d, *J*=7.6 Hz, 7-H), an isolated olefin proton (δ5.79 s, 8-H) and two methyl (δ1.56 s, 21-$\underline{H}_3$ and δ1.26 s, 22-$\underline{H}_3$) groups together with signals due to several olefin or methine and methylene groups (Table 3). The ^{13}C NMR spectrum of **2**, analyzed by the DEPT method, revealed the presence of three amide carbonyls (δ178.52 s, C-2; δ162.60 s, C-11; and δ155.09 s, C-17)[11] and two methyl (δ25.31 q, C-21 and δ18.27 q, C-22) groups along with six sp^2 and two sp^3 methine groups, four sp^2 and a sp^3 quaternary carbons, and three methylene groups (Table 3).

Detailed analyses of the ^1H and ^{13}C NMR spectra of **2** with the aid of ^1H-^1H COSY and PFG-HMQC spectroscopy, coupled with the results of difference NOE experiments and the above structural information, led us to postulate the existence of partial structures A, B and C (Fig. 3) in **2**. This was further confirmed by PFG-HMBC and long-range selective proton decoupling (LSPD)[12] experiments as described below.

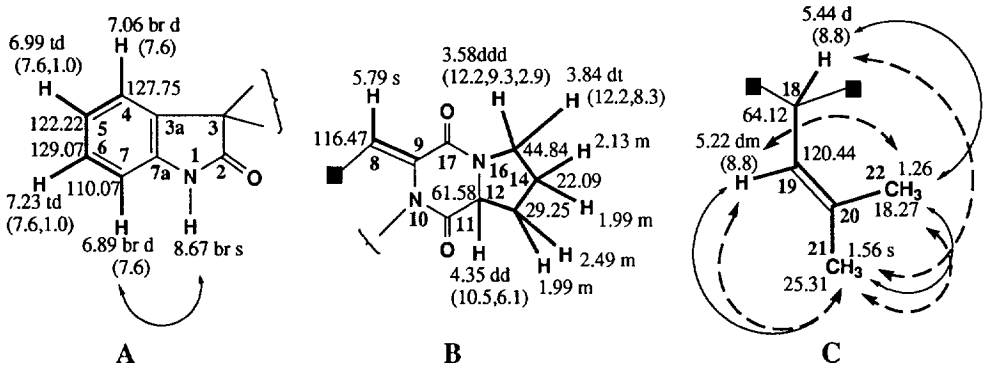

Fig. 3. Partial structures, A, B and C, and NMR data for **2**

Bold lines indicate spin systems obtained by the analyses of ^1H-^1H COSY and PFG-HMQC spectra. Dashed line arrows indicate long-range ^1H -^1H couplings observed in the ^1H-^1H COSY. Solid line arrows indicate NOE's observed in the difference NOE experiments.

In the PFG-HMBC spectrum (Table 3), the quaternary sp^2 carbons at δ127.23 (C-3a) and at δ140.68 (C-7a) showed long-range correlations with the protons 1-H (δ8.67), 5-H (δ6.99) and 7-H (δ6.89) and with the protons 4-H (δ7.06), 6-H (δ7.23) and 7-H in the partial structure A (Fig. 4), respectively, while the amide carbonyl carbon at δ178.52 (C-2) and the quaternary sp^3 carbon at δ61.87 (C-3) showed long-range correlations

Table 3. 500 MHz ^{1}H and 125 MHz ^{13}C NMR data for Spirotryprostatin B (**2**) in chloroform-*d*[a)]

Positions	δ_H (J in Hz)	NOE's[b)]	δ_c	HMBC			$^1J_{CH}$ in Hz[c)]
				2-bonds[d)]	3-bonds[e)]	4-bonds[f)]	
1 (NH)	8.67 br s	7	-------				
2	----		178.52 s	1[g)]	8, 18		
3	----		61.87 s	8, 18	1, 4		
3a	----		127.23 s		1,5,7,8,18		
4	7.06 br d (7.6)	5, 19	127.75 d		6	1	161
5	6.99 td (7.6, 1.0)		122.22 d	6	7		162
6	7.23 td (7.6, 1.0)		129.07 d	7	4		160
7	6.89 br d (7.6)	1, 6	110.07 d	6	5		162
7a	----		140.68 s	1, 7	4, 6		
8	5.79 s		116.47 d		18		184
9	----		138.18 s	8	18		
11	----		162.60 s	12	13β, 18	8	
12	4.35 dd (10.5, 6.1)	13α, 14α	61.58 d	13	14α, 15β		142
13α	2.49 m	12, 13β, 14α	29.25 t	12	14α, 15α		130
β	1.99 m						
14α	1.99 m		22.09 t	13, 15			130
β	2.13 m	13β, 14α, 15β					
15α	3.58 ddd (12.2, 9.3, 2.9)		44.84 t		13α		144
β	3.84 dt (12.2, 8.3)	14β, 15α					
17	----		155.09 s		8, 15β		
18	5.44 d (8.8)	22	64.12 d	19	8		148
19	5.22 dm (8.8)	4, 21	120.44 d	18	21, 22		156
20	----		138.33 s	21, 22	18		
21	1.56 s	19, 22	25.31 q		19, 22		126
22	1.26 d (0.9)	18, 21	18.27 q		19, 21		130

a): Signal assignments were based on the results of ^{1}H-^{1}H COSY, PFG-HMQC, PFG-HMBC and difference NOE experiments. b): Numbers in the column indicate the protons at which NOE's were observed in the difference NOE experiment under irradiation of the proton in the corresponding line. c): Data in the column are values for the direct ^{1}H-^{13}C couplings, which were obtained by the nondecoupled ^{13}C NMR experiments. d), e) and f): Numbers in each column respectively indicate the protons coupled with the carbon through two, three and four bonds, respectively, which were detected by the PFG-HMBC experiments with long-range coupling J_{CH} values of 8.3 and 4 Hz, respectively. When both α-H and β-H in a methylene group showed long-range correlations with the carbon in the PFG-HMBC experiments, only the position number for the protons was given. g): Long-range coupling between 1-H and C-2 was detected in the PFG-HMBC spectrum measured with a long-range J_{CH} value of 4Hz.

with the proton 1-H and with the protons 1-H and 4-H, respectively. Therefore, they were allotted to the carbons C-3a (δ127.23), C-7a (δ140.68), C-2 (δ178.52) and C-3 (δ61.87) in the partial structure A,

respectively, and thus the partial structure A was confirmed (Fig. 4). It should be noted here that the long-range interaction between the amide proton 1-H and the lactam carbonyl carbon C-2 is very weak and the correlation peak could be detected in the PFG-HMBC spectrum measured with a long-range J_{CH} value of 4 Hz. A small value ($^2J_{CH} < 1$) of the long-range coupling constant between 1-H and C-2 was confirmed by the LSPD[12] experiment under selective irradiation at 1-H (δ8.67). For the partial structure B, two amide carbonyl carbons at δ162.60 and at δ155.09 could be distributed to C-11 and C-17 and the quaternary sp^2 carbon at δ138.18 to C-9, respectively, according to the long-range correlations shown by solid line arrows on the partial structure B in Fig. 4. Formation of the five-membered heterocyclic ring by connection of C-12 and C-15 across the nitrogen atom at the position 16 in the partial structure B (Fig. 4) was evidenced by the long-range correlation between C-12 and 15-H_β (δ3.84) in the PFG-HMBC spectrum and by the chemical shift values of C-12 (δ61.58) and C-15 (δ44.84). It is worthy to note here that long-range correlations through four bonds were clearly observed between C-4 and 1-H in the partial structure A and between C-11 and 8-H in the partial structure B, respectively, in the PFG-HMBC spectrum. These are ascribed to the W-form relationships[13] between C-4 and 1-H and between C-11 and 8-H, respectively, and further supported the partial structures A and B. Next, for the partial structure C, the quaternary sp^2 carbon at δ138.33 could be assigned to C-20 according to the long-range correlations between the carbon (δ138.33) and the protons 18-H, 21-$\underline{H}_3$ and 22-$\underline{H}_3$. Also some other long-range correlations confirming the partial structure C are given by solid line arrows on the partial structure C in Fig. 4.

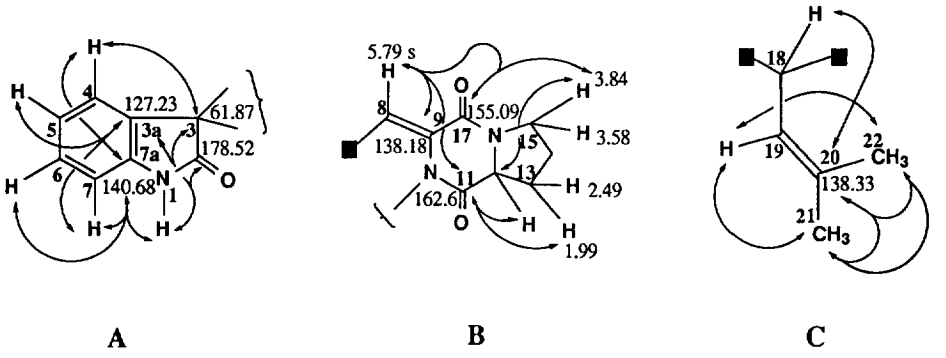

Fig. 4. Partial structures, A, B and C, and NMR data for **2**

Solid line arrows indicate long-range ^1H -^{13}C couplings detected by the PFG-HMBC experiments with the long-range J_{CH} value of 8.3 or 4 Hz, respectively.

Then, the connectivities between the partial structures A, B and C were determined also by extensive analysis of the PFG-HMBC spectrum. As shown in Fig. 5, both the methine protons 8-H in the partial structure B and 18-H in the partial structure C showed long-range correlations with the carbons C-2, C-3 and C-3a in the

partial structure A and the latter 18-H further correlated with the amide carbonyl carbon C-11 in the partial structure B. Therefore, C-8 in the partial structure B and C-18 in the partial structure C could be connected across C-3 in the partial structure A and C-18 be further connected with C-11 across the nitrogen atom at the position 10 in the partial structure B to form a five-membered enamine ring[14]. Thus the planar structure of **2** was deduced (Fig. 5).

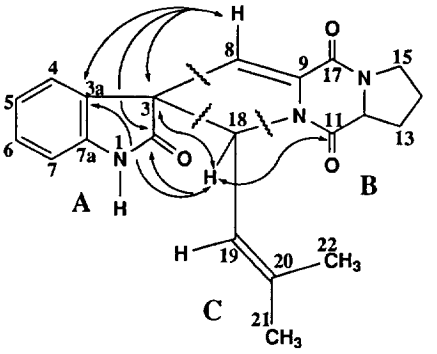

Fig. 5. Planar Structure and NMR data for **2**

Wave lines on the structure indicate the boundary between the partial structures, A, B and C. Solid line arrows indicate long-range ^{1}H -^{13}C couplings detected by the PFG-HMBC experiments with the long-range J_{CH} value of 8.3 or 4 Hz, respectively.

The relative stereochemistry at C-3 and C-18 of **2** in Chart 1, the same as that of **1**, was determined by NOE's observed between 4-H and 19-H in the difference NOE experiments under respective irradiation at 4-H or 19-H. Although executive NMR experiments could not give sufficient information to determine the relative stereochemistry at C-12 in **2**, the co-occurrence of **1** and **2** in the secondary metabolites of *Aspergillus fumigatus* enabled us to propose the proton 12-H in **2** being in the α-direction, the same as that in **1**, from a consideration of the probably same biogenetic origin.

Biological Activities of Spirotryprostatins A (1) and B (2)

Cell cycle inhibitory activities for **1** and **2** were measured by using mouse tsFT210 cells and the bioassay was carried out by the synchronously cultured assay as we have previously reported[5,8]. The tsFT210 cell line is a temperature-sensitive p34^{cdc2} mutant and the cells grew normally at 32°C, but were arrested in the G2 phase at 39°C. The G2-arrested cells by high temperature synchronously passed through M phase to enter into G1 phase when they were transferred to 32°C. Both spirotryprostatins A (**1**) and B (**2**) inhibited the cell cycle progression of tsFT210 cells at the G2/M phase when the G2-arrested cells allowed to pass through M phase to enter into G1 phase by releasing from the temperature-arrest.

Typical flow cytometric histograms for **1** and **2** are given in Fig. 6 and morphological observations of the corresponding cells are also given. Spirotryprostatin A (**1**) could inhibit the most portion of tsFT210 cells in the G2/M phase at a concentration of 253.2 μM (Fig. 6), while spirotryprostatin B (**2**) completely inhibited the cell

cycle progression of tsFT210 cells in the G2/M phase at concentrations over 34.4 μM like as shown in Fig. 6. Half maximal inhibitory concentrations of **1** and **2** were 197.5 μM and 14.0 μM, respctively.

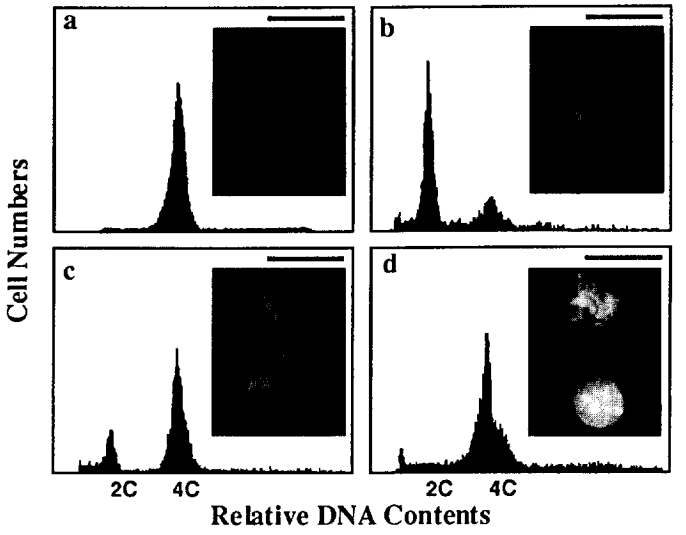

Fig. 6. Effects of **1** and **2** on the cell cycle progression of tsFT210 cells.

tsFT210 cells at a density of $2x10^5$ cells/ml in RPMI-1640 medium supplemented with 5% calf serum were synchronized in the G2 phase by incubation at 39.4°C for 17 hours (a). Then the cells were transferred to 32°C for 4 hours in the absence (b) or in the presence of 253.2 μM of **1** (c) and 34.4 μM of **2** (d), respectively. Photographs show morphological characteristics of the corresponding cells observed under the fluorescence microscope after visualizing the cell nuclei by stain with Heochst 33258 reagent (Bar = 23 μm).

DISCUSSIONS

The present work has provided two novel diketopiperazine alkaloids, spirotryprostatins A (**1**) and B (**2**), as new G2/M phase inhibitors of the mammalian cell cycle. The molecules of **1** and **2** have an unique structural skeleton with a spiro ring system composed from a γ-lactam fused to a benzene ring and a five-membered hetero ring fused to a diketopiperazine moiety, which are composed from a tryptophan unit, a proline residue and an isoprenyl group. The tryptophan unit has been modified by dihydrogenation at C_2/C_3 and further oxidation at C_2 positions in both **1** and **2** and modified further by dehydrogenation at C_8/C_9 positions to form an enamine ring in **2**. Few kinds of spiro compounds belonging to the diketopiperazine series derived from tryptophan and proline residues had so far been known in the nature[15], but none of them had the spiro ring skeleton like as those in **1** and **2**. On the other hand, tryptoquivalines are known as spiro compounds with a spiro ring system composed

from two heterocyclic rings both five-membered[16], but the spiro rings in tryptoquivalines are different at all with those in **1** and **2**. Spirotryprostatins A (**1**) and B (**2**) provide the first example of a novel class of natural diketopiperazines with an unique spiro ring skeleton and the present result provides **1** and **2** as a new inhibitor of the mammalian cell cycle.

To the cell cycle progression of tsFT210 cells, **2** showed stronger inhibitory activity than that of **1**[17]. Previously we have reported[8] that the methoxy group on the benzene ring in tryprostatin A and fumitremorgin C negatively dominated the cell cycle inhibitory activity for those compounds, compared with their demethoxy derivatives, tryprostatin B and demethoxyfumitremorgin C, respectively. The methoxy group in **1** is likely to play also the same role probably in the marked decrease of the inhibitory activity of **1** than that of **2** in view of the structural and biological results in the present study, although the structural difference at C_8/C_9 positions between **1** and **2** might be also a factor should being in a consideration[17].

In morphological observations, a certain portion of the tsFT210 cells treated by **1** and **2** showed morphological characteristics of the condensed chromosomes, which are typical of the M phase cells, and some others appeared with morphological characteristics of the G2 phase cells (Fig. 6). This means that the tsFT210 cells treated by **1** and **2** are trapped both in G2 and M phases. Incidently, the portion of G2 cells are increased dose-dependently in the tsFT210 cells treated by **1** and **2** (data not shown).

Detailed studies on their action mechanisms are currently being undertaken.

EXPERIMENTAL SECTION

General Instrumental Analyses

Melting points were measured using a Yanagimoto micro melting point apparatus and were uncorrected. Optical rotations were determined in $CHCl_3$ solutions on a JASCO DIP-370 polarimeter. UV spectra were taken with a Hitachi 220A spectrophotometer in MeOH solutions and IR spectra were recorded on a Shimadzu FTIR-8100M Fourier transform infrared spectrophotometer in KBr discs. EI-MS (ionization voltage, 70 eV, accelerating voltage, 3 kV) and HR-EI-MS were measured respectively on Hitachi M-80A and Hitachi M-80 mass spectrometers using a direct inlet system. ^1H and ^{13}C NMR spectra were taken on a JEOL GSX-500 or α-400 spectrometer with tetramethylsilane as an internal standard and chemical shifts are recorded in δ values. Multiplicities of ^{13}C NMR signals were determined by the DEPT method and are indicated as s (singlet), d (doublet), t (triplet) and q (quartet). 2D NMR spectra (^1H-^1H or PFG ^1H-^1H COSY, PFG-HMQC and PFG-HMBC spectra) were measured on a JEOL GSX-500 or α-400 spectrometer by the use of JEOL standard pulse sequences and collected data were processed by JEOL standard software. Difference NOE spectra were obtained by the use of a JEOL standard pulse sequence with irradiation for 5 seconds.

Conditions for Isolation of the Diketopiperazines

TLC was done on pre-coated silica gel 60 F_{254} plates (0.25 mm thick, 20 x 20 cm, Merck) and the spots were detected under UV lights (254 and 365 nm) or by the use of 10% aqueous sulfuric acid reagent. Silica gel

60 (230-400 mesh, Merck) and reversed phase silica gel SSC ODS-7515-12A (Senshu Scientific Co. Ltd., Japan) were used for open column chromatography and preparative middle pressure liquid chromatography, respectively.

Analytical HPLC was carried out on a reversed phase column (CAPCELL PAK C-18 or C-8, 4.6 x 250 mm, Shiseido Co., Japan) by the use of a HPLC equipment with a Hitachi L-6000 pump and a Waters 991J photodiode array detector system under a flow rate of 1 ml/min. Preparative HPLC and preparative middle pressure liquid chromatography were performed on a HPLC system equipped with a Hitachi L-6000 pump and a SSC UV detector. CAPCELL PAK C-18 and C-8 columns (20 x 250 mm, Shiseido) were used in the preparative HPLC, and MMC-1-30-300 glass column (30 x 300 mm, Kyoushin Industry Co., Japan) packed with reversed phase silica gel SSC ODS-7515-12A were used for preparative middle pressure liquid chromatography.

Fermentation of the Producing Fungal Strain

The producing fungal strain, *Aspergillus fumigatus*, on a potato dextrose agar slant was inoculated into a 500-ml cylindrical flask containing 100 ml of the seed medium consisting of glucose 3%, soluble starch 2%, soybean meal 2%, K_2HPO_4 0.5%, $MgSO_4 \cdot 7H_2O$ 0.05% (adjusted to pH 6.5 prior to sterilization) and cultured at 28°C for 27 hours on a rotary shaker at 300 rpm. The culture was transferred into 18 liters of the seed medium with 0.05% of antifoam reagents CA-123 and KM-68, respectively, in a 30-liter jar fermenter. Further fermentation for seed culture was carried out at 28°C for 24 hours with an agitation rate of 350 rpm and an aeration rate of 9 liters/minute.

Then the producing fermentation was carried out in a 600-liter jar fermenter containing 400 liters of the production medium having the same composition of the seed medium with 0.05% of antifoam reagents CA-123 and KM-68, respectively. The seed culture (18 L) was transferred into the 600-liter fermenter and the fermentation was performed at 28°C for 66 hours with an agitation rate of 350 rpm and an aeration rate of 200 liters/min.

Separation of the Fermentation Broth

The whole broth (410 L) was filtrated to separate to a broth supernatant (370 L) and a mycelial cake. The former was extracted once with 400 L of EtOAc to give an EtOAc solution and the latter was extracted with 90% aqueous acetone (400 L x 1 time) which was evaporated *in vacuo* to remove acetone to give an aqueous solution (60 L). The aqueous solution was extracted with EtOAc (120 L x 2 times) to afford 220 L of EtOAc solution. Both the EtOAc solutions obtained were combined and concentrated *in vacuo* to give an oily extract (1.2 L). To the oily extract, 1.2 L of *n*-hexane was added, and the extract was suspended by stirring followed by sonication for 10 minutes and then the *n*-hexane-insoluble part was obtained by centrifugation at 6000 rpm for 20 minutes. The *n*-hexane-insoluble part was treated two more times with *n*-hexane (1.2 L x 2) by the same manner to remove nonpolar oil fraction. To the *n*-hexane-insoluble part obtained, $CHCl_3$ (1.2 L) was added and suspended by sonication for 10 minutes and then centrifuged for 20 minutes at 6000 rpm to obtain a $CHCl_3$ solution. The

$CHCl_3$-insoluble part was extracted one more time with $CHCl_3$ (1.2 L) by the same manner, and both the $CHCl_3$-solutions obtained were combined and concentrated under reduced pressure to afford a $CHCl_3$-soluble syrup. This was treated once more with *n*-hexane (1.2 L) as described above to give a *n*-hexane-insoluble part which was partitioned between $CHCl_3$-H_2O. The $CHCl_3$ solution obtained was concentrated under reduced pressure to give an active $CHCl_3$ extract (66 g) as powders.

The $CHCl_3$ extract (66 g) was solved in 250 ml of *n*-hexane-$CHCl_3$ (20:80) solution and subjected to a silica gel column packed in *n*-hexane (silica gel, 1500 g; bed volume, 7.5 x 75 cm; retention volume, 3 L). The column was then eluted successively with *n*-hexane-$CHCl_3$ [50:50 (7.5 L)→ 25:75 (13.7 L)→ 10:90 (9.5 L)] solution, $CHCl_3$ (1.2 L) and $CHCl_3$-MeOH [99.5:0.5 (9 L)→ 99:1 (1.2 L)→ 98:2 (6 L)→ 96:4 (9 L)→ 90:10 (9 L)→ 80:20 (10 L)→ 70:30 (6 L)] solution, respectively. After elution with 7.5 L of *n*-hexane-$CHCl_3$ (50:50) solution which was collected in a portion, the eluate was collected in each 3 L portion, monitored by TLC, combined and concentrated *in vacuo* to give twenty five fractions [**Fr.1**, *n*-hexane-$CHCl_3$ (50:50) eluate; **Fr.2-Fr.4**, *n*-hexane-$CHCl_3$ (25:75) eluate; **Fr.5-Fr.6**, *n*-hexane-$CHCl_3$ (10:90) eluate; **Fr.7**, *n*-hexane-$CHCl_3$ (10:90) & $CHCl_3$ eluate; **Fr.8-Fr.10**, $CHCl_3$ eluate; **Fr.11**, $CHCl_3$ & $CHCl_3$-MeOH (99.5:0.5) eluate; **Fr.12-Fr.13**, $CHCl_3$-MeOH (99.5:0.5) eluate; **Fr.14**, $CHCl_3$-MeOH (99.5:0.5 & 99:1) eluate; **Fr.15-Fr.17**, $CHCl_3$-MeOH (99:1) eluate; **Fr.18-Fr.20**, $CHCl_3$-MeOH (98:2) eluate; **Fr.21-Fr.22**, $CHCl_3$-MeOH (96:4) eluate; **Fr.23**, $CHCl_3$-MeOH (96:4 & 90:10) eluate; **Fr.24** $CHCl_3$-MeOH (90:10) eluate; **Fr.25** $CHCl_3$-MeOH (80:20 &70:30) eluate].

Isolation of Spirotryprostatins and Other Diketopiperazines

The fraction **Fr.7** (0.76 g) eluted by *n*-hexane-$CHCl_3$ (10:90) & $CHCl_3$ solutions from the silica gel column was recrystallized from MeOH to give **demethoxyfumitremorgin C** (141 mg) as pale yellow needles. The mother MeOH solution was separated by preparative HPLC on a CAPCELL PAK C-18 column using MeOH-H_2O (60:40) as eluting solvent (detector wave length, 210 nm; flow rate, 10 ml/min) to give an active fraction **fr.5** [retention time (Rt)=13 min, 32 mg], **tryprostatin B** (Rt=21 min, 64.4 mg) and **demethoxyfumitremorgin C** (Rt=30 min, 18.6 mg), respectively. The fraction **fr.5** was further subjected to a HPLC separation on a CAPCELL PAK C-8 column with MeOH-H_2O (40:60) eluting solution (detector wave length, 210 nm; flow rate, 10 ml/min) to give **spirotryprostatin B** (**2**, Rt=70.6 min, 11 mg) as a pale yellow crystalline solid from a MeOH solution.

The fraction **Fr.8** (3.5 g) eluted by $CHCl_3$ from the silica gel column was recrystallized from MeOH to give **fumitremorgin C** (345.5 mg) as pale yellow needles. The mother MeOH solution portion was separated by repeated preparative middle pressure liquid chromatography (detector wave length, 300 nm; flow rate, 35 ml/min) using MeOH-H_2O (60:40 or 50:50) eluting solvent to give **tryprostatin A** (1048 mg) and **fumitremorgin C** (458 mg) as pale yellow needles from MeOH, respectively.

The fraction **Fr.14** (0.99 g) eluted by $CHCl_3$-MeOH (99.5:0.5 & 99:1) solvents from the silica gel column

was separated by preparative HPLC on a CAPELL PAK C-18 column using MeOH-H_2O (60:40) as eluting solvent (detector wave length, 220 nm; flow rate, 10 ml/min) to give crude **spirotryprostatin A** (**1**, Rt=17 min; 2.1 mg) which was further purified by repeated HPLC under the same condition to give 1.2 mg of pure **1** as pale yellow amorphous powders from a MeOH solution.

Bioassay for Cell Cycle Inhibitory Activity

The tsFT210 cells were routinely maintained at 32°C in RPMI-1640 medium supplemented with 5% calf serum (HyClone Inc., Logan, UT, USA) in the presence of 30 μg/ml of penicillin and 42 μg/ml of streptomycin under a humidified atmosphere of 5% CO_2 and 95% air. The cells were arrested in the G2 phase by incubation at 39.4°C for 17 hours and the cells were allowed to pass through M phase to enter into G1 phase by incubation at 32°C for 4 hours after treatment with the samples. Then distribution of the cells within cell cycle were determined by flow cyctometry as we have previously reported[8].

ACKNOWLEDGEMENTS

We thank Ms. Tamiko Chijimatsu (RIKEN) for the measurements of PFG-HMBC spectra. This research work was supported in part by a Grant for "Biodesign Research Program" from RIKEN (C.-B. Cui and H. Osada) and a Grant from Ministry of Education, Japan.

REFERENCES AND NOTES

1. A part of this work was reported in our preliminary communication. C.-B. Cui, H. Kakeya and H. Osada, *J. Antibiot.*, **1996**, 49 (8), in press.
2. J. A. Cooper and B. Howell, *Cell*, **1993**, 73, 1051-1054.
3. R. A. Weinberg, *Science*, **1991**, 254, 1138-1146.
4. B. Alberts, D. Bray, J. Lewis, M. Raff, K. Roberts and, J. D. Watson, *Molecular Biology of the Cell*; Second Edition, Glarland Publishing, Inc.: New York, **1989**; pp. 752, pp. 1199 and pp. 1203.
5. H. Osada, C.-B. Cui, R. Onose and F. Hanaoka, *Bioorg. Med. Chem.*, **1996**, in press.
6. C.-B. Cui, H. Kakeya, G. Okada, R. Onose, M Ubukata, I. Takahashi, K. Isono and H. Osada, *J. Antibiot.*, **1995**, 48, 1382-1384.
7. C.-B. Cui, M. Ubukata, H. Kakeya, R. Onose, G. Okada, I. Takahashi, K. Isono and H. Osada, *J. Antibiot.*, **1996**, 49, 216-219.
8. C.-B. Cui, H. Kakeya, G. Okada, R. Onose and H. Osada, *J. Antibiot.*, **1996**, 49, 527-533.
9. C.-B. Cui, H. Kakeya and H. Osada, *J. Antibiot.*, **1996**, 49, 534-540.
10. C. N. R. Rao, *Chemical Applications of Infrared Spectroscopy*; Academic Press Inc.: New York, **1963**; pp. 258-261.
11. The ^1H and ^{13}C NMR spectra of tryprostatin B (demethoxytryprostatin A) and demethoxyfumitremorgin C were closely resembled those of tryprostatin A and fumitremorgin C, respectively, except for the signals due to the aromatic ring moieties (*cf.* reference 9). In the case of **2**, however, both electronic and stereochemical affects from the double bond at the C_8/C_9 positions might be arisen and probably be a main

reason causing changes of both ^{1}H and ^{13}C NMR signal patterns comparing with those of **1**. For instance, two amide carbonyl carbons in the diketopiperazine part in **2** appeared in the markedly high field region (δ162.60, C-11 and δ155.09, C-17) than the corresponding carbons in **1** (Table 2), tryprostatins and related diketopiperazine alkaloids (*cf.* reference 9).

12. a) S. Takeuchi, J. Uzawa, H. Seto and H. Yonehara, *Tetrahedron Lett.*, **1977**, 2943-2946. b) H. Seto, T., Sasaki, H. Yonehara and J. Uzawa, *Tetrahedron Lett.*, **1978**, 923-926. c) H. Seto, N. Otake, M. Koyama, H. Ogino, Y. Kodama, N. Nishizawa, T. Tsuruoka and S. Inoue, *Tetrahedron Lett.*, **1983**, 24, 495-498.
13. a) C.-B. Cui, Y. Tezuka, T. Kikuchi, H. Nakano, T. Tamaoki and, J.-H. Park, *Chem. Pharm. Bull.*, **1992**, 40, 2035-2040. b) H.-O. Kalinowski, S. Berger and S. Bran, *Carbon-13 NMR Spectroscopy*; John Wiley and Sons: New York, **1988**; pp. 543. c) H. Seto, K. Furihata, N. Otake, Y. Itoh, S. Takahashi, T. Haneishi and M. Ohuichi, *Tetrahedron Lett.*, **1984**, 25, 337-340.
14. It is noteworthy that the C_8 sp^2 methine in **2** had a quite larger $^{1}J_{CH}$ coupling constant (184 Hz) than those (Table 3) of the other sp^2 methines in **2**, which is also larger than those (about 170 Hz) of the corresponding methins in general five-membered hetero rings containg a nitrogen atom. This supported also the structural skeleton deduced for **2**, in where electronegative substituents on or around the double bond at C_8/C_9 positions, especially the C-17 carbonyl linked to C-9, probably resulted in an increase in the $^{1}J_{CH}$ coupling constant of the C-8 methine group.
15. a) P. S. Steyn, *Tetrahedron*, **1973**, 29, 107-120. b) P. S. Steyn, *Tetrahedron Lett.*, **1971**, 3331-3334. c) A. J. Brich and J. J. Wright, *Tetrahedron*, **1970**, 26, 2329-2344. d) R. M. Williams, E. K. H. Coffman and T. Glinka, *J. Am. Chem. Soc.*, **1989**, 111, 3064-3065.
16. P. S. Steyn and R. Vleggaar, *Progress in the Chemistry of Organic Natural Products* (Founded by L. Zechmiester, Edited by W. Herz, H. Grisebach and G. W. Kirby). **1985**, 48, 1-80.
17. Incidentally, tryprostatins A (TPS-A), B (TPS-B), fumitremorgin C (FT-C) and demethoxyfumitremorgin C (DMFT-C) inhibited the cell cycle progression of tsFT210 cells at the M phase with IC_{50} values of 78.7 μM for TPS-A, 18.8 μM for TPS-B, 14.0 μM for FT-C and 1.78 μM for DMFT-C, respectively (*cf.* reference 8). Spirotryprostatin B (**2**) had the IC_{50} value of 14.0 μM, being in the same order with those of the above compounds, while the IC_{50} value (197.5 μM) for spirotryprostatin A (**1**) is one order lager than those of **2** and the above compounds. To a certain extent, ratio of the IC_{50} values for TPS-A/TPS-B (78.7/18.8=7.9) and for FT-C/DMFT-C (14.0/1.78=4.2) might indicate the strength of negative effect of the methoxy group in those compounds on the cell cycle inhibitory activity, respectively, and the difference between the values (7.9 for TPS-A/TPS-B and 4.2 for FT-C/DMFT-C) might reflect the difference in the structural skeleton between two groups of those compounds. The ratio of IC_{50} values between **1** and **2** (197.5/14.0=14.1) is quite larger than those of the above compounds, in which the contributions from the different structural skeleton and an affection from the structural difference at the C_8/C_9 positions between **1** and **2** might be involved except for the effect of methoxy group in **1**.

(*Received in Japan* 12 *July* 1996; *accepted* 5 *August* 1996)